SEE
Measurement as Process

Paul G. Plöger

Djordje Vukcevic

Outline

General remarks (on ALL of SEE)

1 Introduction / Motivation

2 Foundations

- **2B**asic Terms and definitions
- **2E**rrors
- **2D**istributions

3 Summary

Labwork

General: Target

Learn how to **design** experiments decently

Learn how to **conduct** experiments decently

Learn how to **describe the results** decently (a.k.a. in a scientifically sound way)

1 Some recent BAD Examples

4,8376 +/- 0.1

	Precision	Recall	Time taken (s)
Instantanuous diagnosis			
Control run	-	-	1
Exogenous Intervention run	1	1	1
Progressive diagnosis			
Control run	-	-	1
Exogenous Intervention run	1	1	1

TABLE 6.1: Calculated precision and recall of exogenous intervention diagnosis in a simulated youbot. The calculation was done on a specific time interval when the exogenous interventions was occurring.

	Assigned positive	Assigned negative
Actual positive	60	12
Actual negative	48	0

Table 5.2: Error matrix for PADI dataset

	Assigned positive	Assigned negative
Actual positive	103	4
Actual negative	13	0

Table 5.3: Error matrix for NUS dataset-I

$$s = \frac{1}{2} a * t^2 \Rightarrow s = \frac{1}{2a} * a^2 * t^2 \overset{v=a*t}{\Longrightarrow} s = \frac{1}{2a} * v^2 \Rightarrow v = \sqrt{s\ *\ 2a}$$

Abbildung 30: Herleitung der Formel zur Geschwindigkeitsberechnung

Da diese Geschwindigkeit, je nach zufahrender Distanz, die maximale Geschwindigkeit des Motors um ein Vielfaches übersteigen kann, ist ein Vergleich mit dieser sinnvoll. Um ein zu abruptes Anfahren des Motors zu verhindern, wird dieser mit einer konstanten Beschleunigung geregelt. Um diesen Faktor nicht auszuhebeln, wird die Geschwindigkeit auch mit diesem Wert verglichen (siehe Abbildung 31).

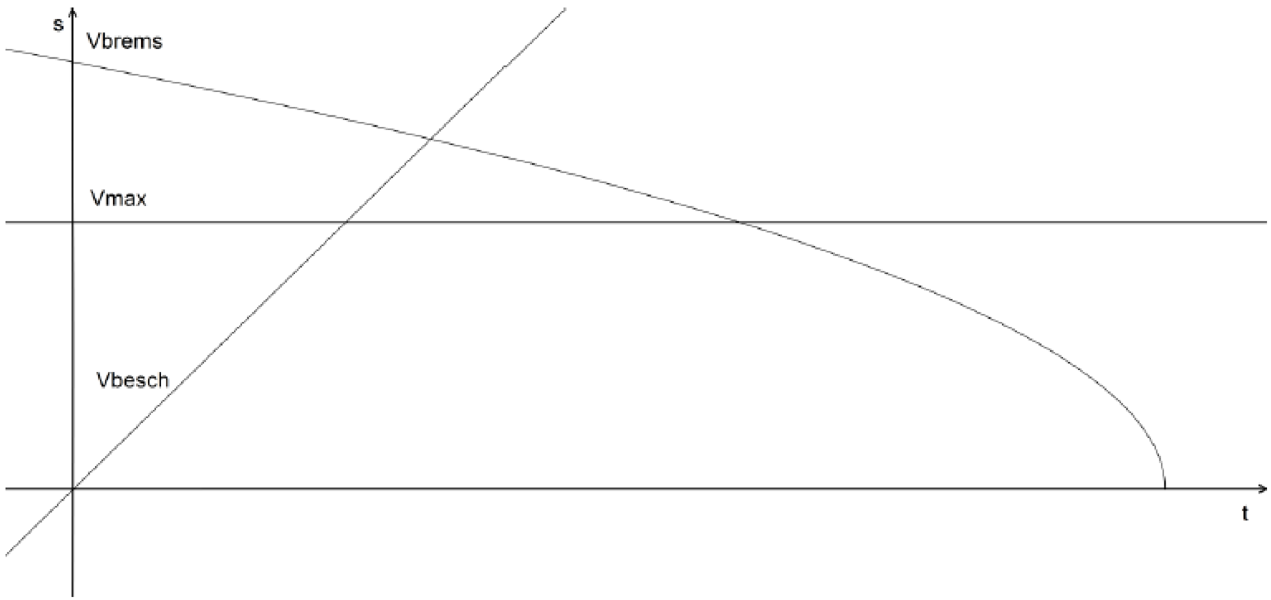

Abbildung 31: Ermittlung der zu fahrenden Geschwindigkeit

Daraus ergibt sich eine Formel für die zufahrende Geschwindigkeit (siehe Abbildung 32).

$$v = \min(Vmax, Vbeschleunigt, Vgebremst)$$

Abbildung 32: Formel zur Ermittlung der zufahrenden Geschwindigkeit

1 General: Knowledge areas

- Theory of Measurement (“Messwerterfassung”)
- Mathematics
  - Probability theory
  - Statistics
- Physics
  - Instrumentation

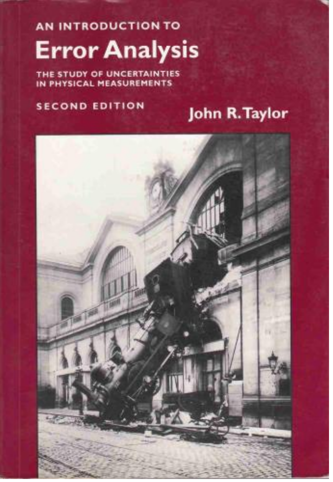

1 Reading results from experiments

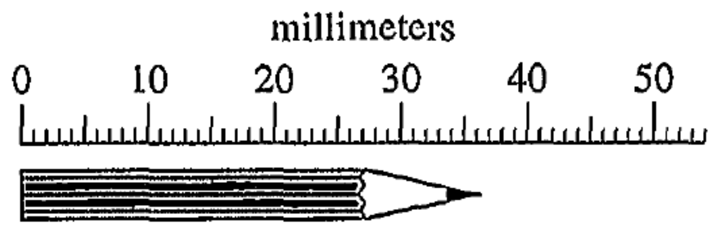

Figure 1.2. Measuring a length with a ruler.

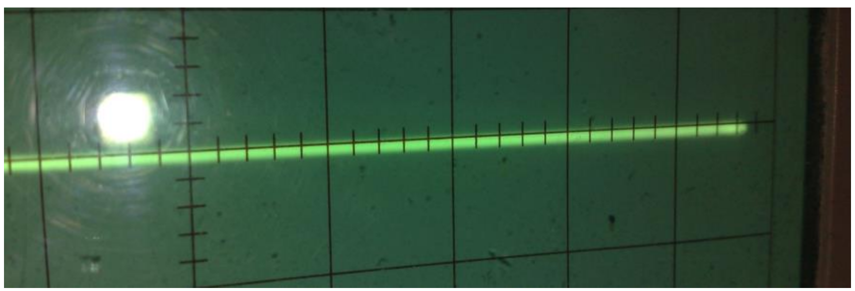

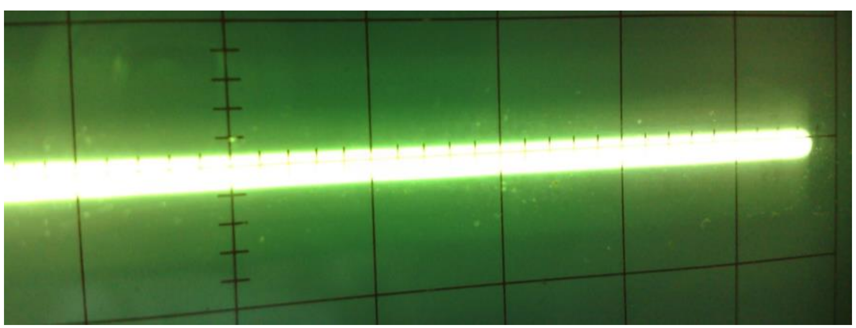

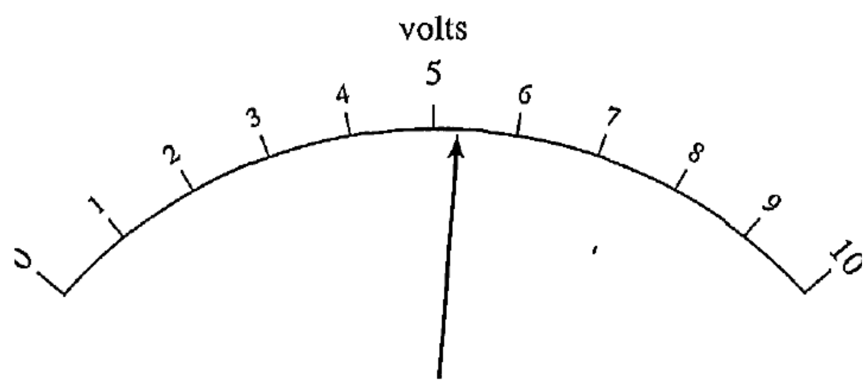

Figure 1.3. A reading on a voltmeter.

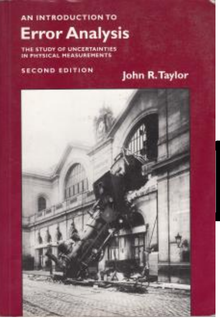

1 Best Estimate ± Uncertainty

E.g.: measured value of time = 2.4 ± 0.1 s.

(measured value of x) = $x_b \pm \delta x$

x_b : experimenter‘s best estimate

δx: uncertainty, error, margin of error (it‘s > 0)

i.e. confidence, that x lies in range
$x_b - \delta x$ and $x_b + \delta x$

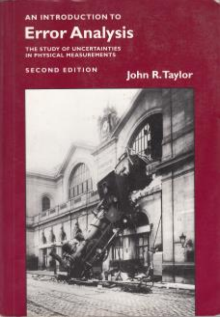

1 Rules for Stating the Uncertainties

e.g. measure the acceleration of gravity g:

(measured g) = 9.82 ± 0.02~~385~~ m/s²

?

Experimental uncertainties should almost always be rounded to ONE significant figure

e.g.: **(measured g) = 9.82 ± 0.02 m/s²**

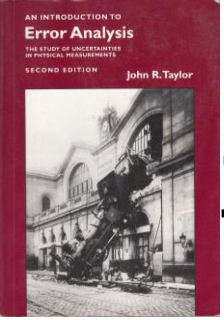

1 Rules for Stating the Answers

After uncertainty in measurement => significant figures in the measured value must also be considered.

e.g.: **measured speed = ~~6051.78~~ ± 30 m/s**

The uncertainty of 30 means that the digit 5 might really be as small as 2 or as large as 8. Clearly the trailing digits 1, 7, and 8 have no significance at all and should be rounded

The **last significant figure** in any stated answer should usually be of then **same order of magnitude** (in the same decimal position) as the uncertainties

measured speed = 6050 ± 30 m/s

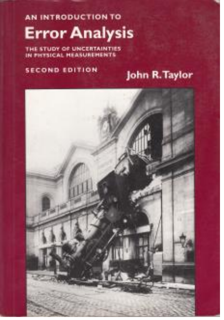

1 Examples

92.81 with an uncertainty of **0.3** ⇒ **92.8** ± 0.3

92.81 with an uncertainty of **3** ⇒ **93** ± 3

92.81 with an uncertainty of **30** ⇒ **90** ± 30

Observe:

To reduce inaccuracies caused by rounding, **any numbers to be used in subsequent calculations** should normally **retain at least one significant figure more** than is finally justified. At the end of the calculations, the **final answer should be rounded** to remove these extra, insignificant figures.

1 Quick check (10min)

Rewrite each of the following measurements in its most appropriate form:

a) $v = 8.123456 \pm 0.0312$ m/s

b) $X = 3.1234 * 10^{4} \pm 2$ m

c) $m = 5.6789 * 10^{-7} \pm 3 * 10^{-9}$ kg.

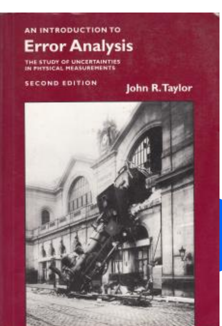

General: Overview

PGP	30.09.13	lecture	Measurement as process
		Testat:	-none-
PR+PGP		Lab class	Run robots on sheet of paper, record distributions
you		Homework	Evaluate data, Do the fit
PR	07.10.13	lecture	Sample solution for 30.09.13
PGP+BK		Testat:	successfull Reprodution a normal distribution in 2D and proof that what you observed is actually a normal distribution, error analysis
PGP+BK		Lab class	read Zhang paper, explain it to newbies in Vision and projective geometry
you		Homework	finish undestanding of Zhang paper
PGP+BK	14.10.13	lecture	Intrinsic / extrinsic camera parameters, radial distortions, calibration
		Testat:	-none
PGP+BK		Lab class	run the CALTECH sw, do the calibration images, find intrisic / extrinsic params for your camera
you		Homework	Read Thrun / Probabal. Robotics / chapter 5.1, 5.2, 5.3
BK	21.10.13	lecture	Sampling of distributions and forward / backward model (Use of Prob. Models in mobile robotibs)
PR+BK		Testat:	correct intrinsic / extrinsic camera matrixes (compare on class level)
PR		Lab class	run the V,\omega experiemtent
		Homework	read 2 articles: On the repseentation and estimation of spatial uncertainty // Location estimation und uncertainty analysis for mobile robots
PGP	28.10.13	lecture	Covariance matrices and error propagation
		Testat:	-none
PR		Lab class	complete the experiment
you		Homework	Read Thrun / Probabal. Robotics / chapter 5.4, 5.5, 5.6
	04.11.13	lecture	-none
PGP+BK		Testat:	good v,\omega model für robot
PR		Lab class	do the ODOmetry Modion model // ticks_left ticks_right
you		Homework	Read Thrun / Probabal. Robotics / chapter 6

1: Oscilloscope experiment

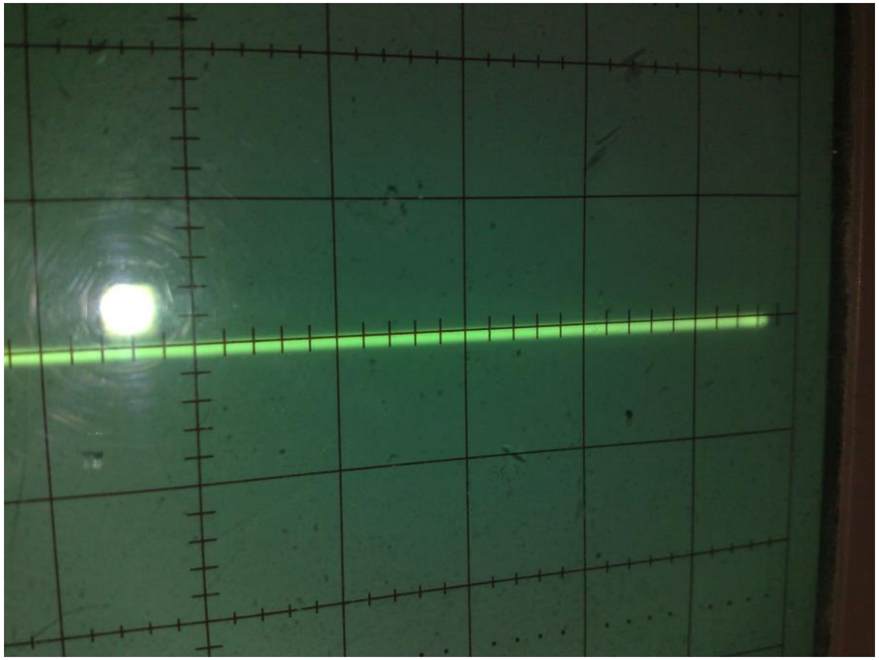

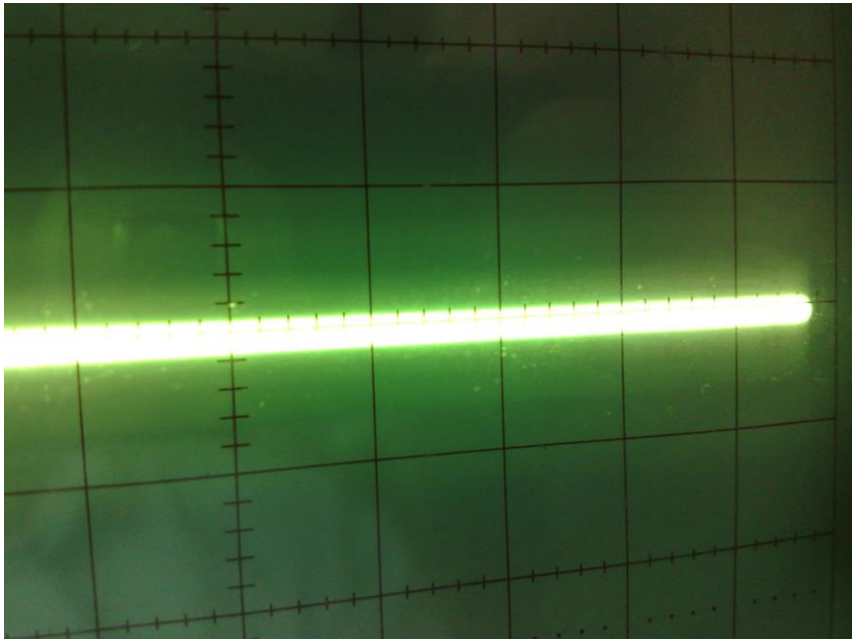

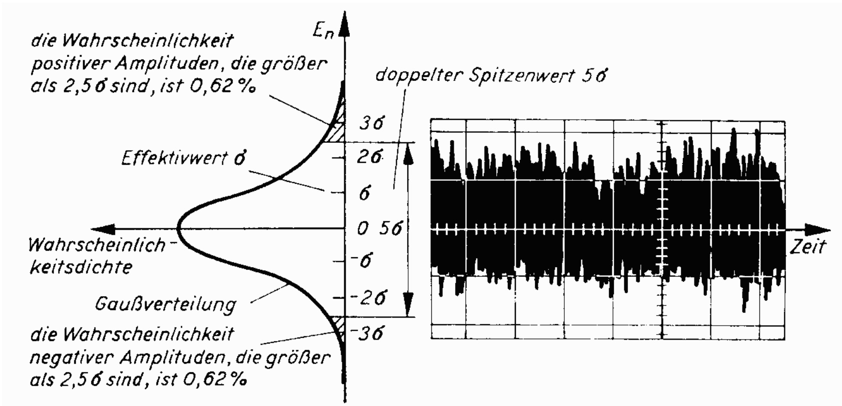

1: Questions

What is the true value (x_t) ?

Can we catch it “exactly”? Why, why not?

If not catchable, how can we sure there *IS* a true value?

How to approximate it best, what is it?

How can we be sure that the measuring instrument did not add (too much) distortion? (called „burden“)

How to validate that the observed values actually follow a distribution? Which?

How to formalize the process as such?

How to interpret the measurement action in physical terms?

1: needed Sciences

Mathematics

- errors: absolute, relative, systematic, random, round off
- (Random variables)
- (Probability distributions)

Statistics

- Empirical mean value
- (Maximum likelihood estimation)
- Statistical tests

Physics / System Theory

- (Burden of instrument)
- (Equivalent circuit diagram)
- Measurement as signal flow graph

2B: System theory: Measuring System

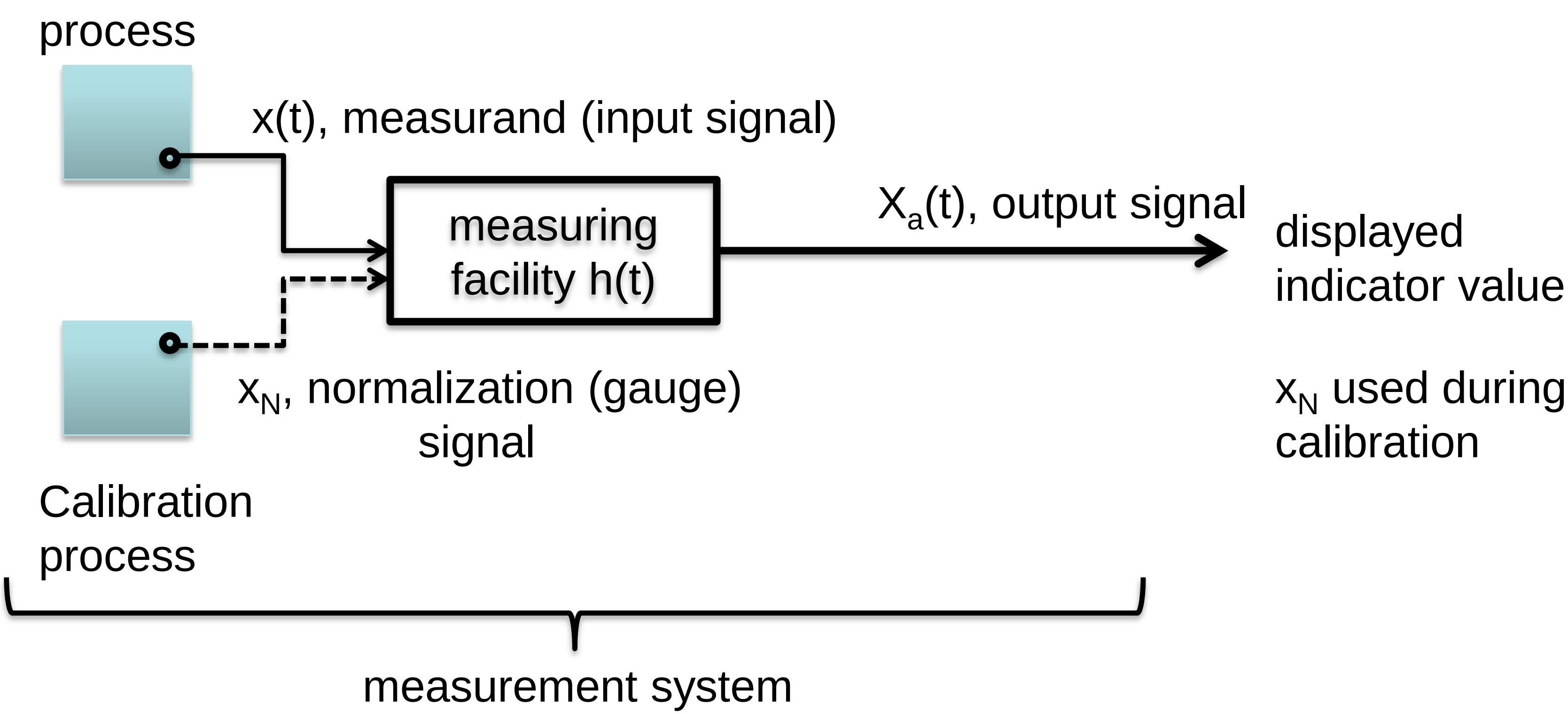

$x(t)$ == measurand

$h(t)$ == transfer function of measuring facility (linear) =>

$x_a(t) = h(t) * x(t)$

2B: Formalization general terms

Measurand:
The measurand is **physical quantity, which is to be quantified** by the measurement (e.g. length, pressure, electrical resistance, etc.).

Measurement:
To „measure" in the strict sense is, to **determine the size of a variable as a multiple** of a to be determined generally recognized unit size of the same physical dimension through **experimental comparison** with a solid measure of this unit.

To „measure" in wider sense is, to **determine experimentally** a quantitative information of a particular property of a test object, which **may be derived from one or more measurable quantities of this test object**. This property may be a size (for example of a force or efficiency), or a mapping (for example a development over time). This property can also describe a system state, characterized via several variables which are recorded in parallel.

e.g. Special case of Measurement: Count
Counting is to **determine the number of elements** (e.g. piece count) or events (e.g. RPM). The count represents a special case of measurement.

e.g. Special case of Measurem.: Inspection
Inspecting means to determine experimentally whether a **particular property of a test piece corresponds to the specified requirements**. If the check is carried out via measuring, it can be considered a special form of measurement .

Display:
The **indicator shows the numerical value** of the to be measured variable. In analog displays one has to determine the **state of the indicator (arrow) on the scale by „reading"**. In digital displays it can be read directly as a number.

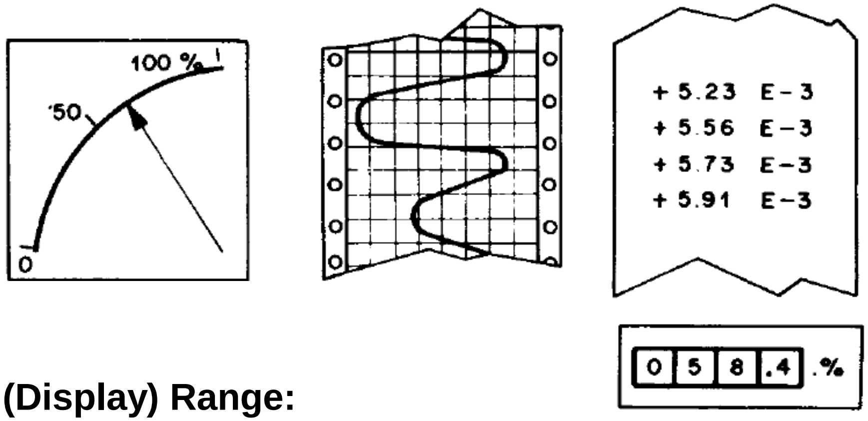

(Display) Range:
The display range of a measuring device is that range of **measured values, which can be read from the scale of the display (full scale, upper limit)**

Measurement range:
The range is that part of the display area for which the **error remains within a guaranteed or prescribed limit of error.**

Displacement range:
The Displacement range is that **area of measured value above which the display of the measuring device starts**.

2B: Formalization general terms

Measured (Quantity) Value :

This is the **value of a specific variable. It will be determined from the displaying measuring instruments by reading this display and building the product of measured value and the unit of the measurand** (eg 3m). It can also be output in the form of a transferable measurement signal and may be sent for further automatic processing (storage, value processing, control, etc.).

Measurement result:

The measurement result is obtained **in general from several measured values by the help of a predetermined relationship**. In the simplest case, a single measurement is already the measurement result.

Device Under Test (DUT):

The DUT is **that part of a physical system, which carries the measurement variable** .

Measurement facility:

The measuring facility is **the entirety of device components used for the purpose of the measurement**. This includes sensor for detection of the measured quantity, amplifiers, computing devices and the output devices to display the observed value and possibly other components.

Measurement System:

The measurement system includes not only the measuring facility but also **those areas of the physical system which contains the DUT, which do affect the measurement process,** in particular the data acquisition .

Meter:

The meter is a either a part or the whole of the measuring facility.

Measuring Principle:

The principle of measurement is **defined as the characteristic physical phenomenon which is used during the measurement** (for example, measurand: temperature, measurement principle: linear expansion, or thermoelectric effects, etc.).

Measuring method:

Understand by this the kind of application or **implementation of the Measurement Principle**. In addition it may mean the function of the measuring device .

Sensitivity:

The Sensitivity is the **indicator pathway on the scale (in mm) per unit of the variable**. In light pointer devices, the vector length is defined as 1m. In digital instruments, the sensitivity is equal to the number of digits per unit of measured quantity. For non-linear meters the sensitivity is a function of the measured value or the display respectively.

Title: Modelling the Indentation Force Response of Non-Uniform Soft Tissue using a Recurrent Neural Network

Rohan Nowell1, Bijan Shirinzadeh2, Julian Smith3 and Yongmin Zhong4

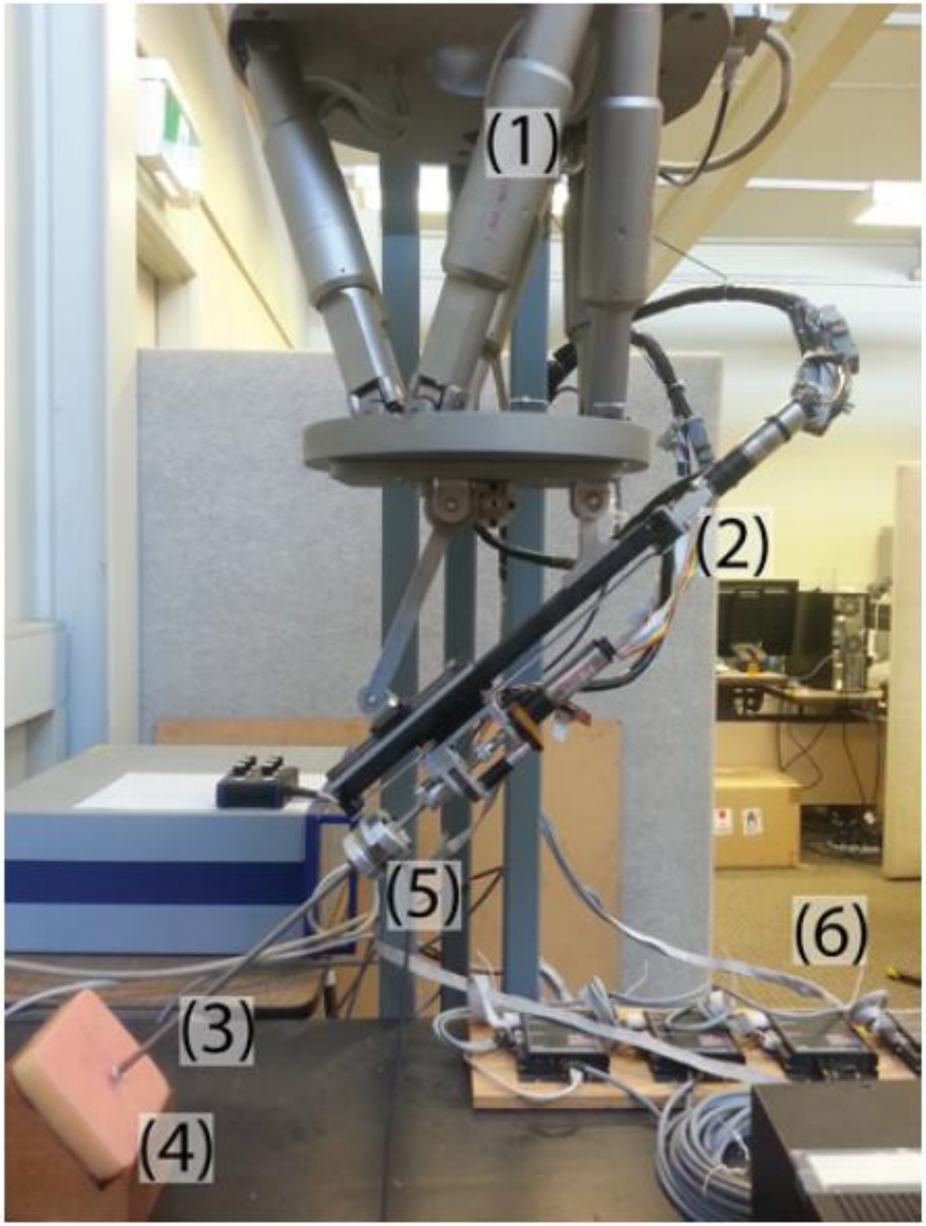

Fig. 2. The experimental research facility for measuring tissue forces. This facility combines the following components: (1) PI Hexapod, (2) monocarrier drive, (3) indentation tool, (4) Simulab complex tissue model, (5) ATI Mini40 force sensor and (6) EPOS2 motor controllers.

II. Experimental Facility

The research facility used to generate the experimental reference and test data is shown in figure 2. The facility contains a 10 DOF robotic system designed and developed for laparoscopic surgery research [24] consisting of a Physik Instrumente Hexapod (1) with an attached monocarrier drive (2). The Hexapod is used to move the indenter (3) over a grid of locations on the tissue analogue (4) while the monocarrier is used to provide the motion in the indentation direction. The indenter contains a force torque (FT) sensor (5) which provides axial force measurements.

The FT sensor is an ATI Mini40 which has a specified unfiltered axial force resolution of 0.04 N. The force measurements are read using a NI DAQ which operates at a rate of 1 kHz. Software filtering is then performed to reduce the high frequency noise and sensor drift is mitigated by periodically zeroing the FT sensor between indentation test locations. The monocarrier is controlled using an EPOS2 motor controller (6) which provides motor position and velocity readings every 4 ms.

The tissue analogue is a Simulab complex tissue model. Damage to the tissue sample from penetration testing has caused it to have a very non-uniform force response over its surface, making it ideal for testing the soft tissue models.

III. Experimental Procedure

The force response data to be modelled was taken by pressing the indenter (6.5 mm hemispherical tip) into the tissue model in the surface normal direction up to a depth of 11.5 mm (38% of the sample depth).

The process for taking the experimental data was as follows: The indenter was moved towards the first grid location above the sample, then an indentation depth is chosen between 0 and 11.5 mm. The indenter is moved to this indentation depth before another depth is randomly chosen. 800 random depth indentations were performed in succession at each of the 25 grid locations on the tissue sample with no material preconditioning. This was done to ensure that a wide array of conditions exist in the training and test data for the neural network models to develop a model which can generalise well. The axial force and the indentation depth were recorded at approximately 4 millisecond intervals. The measured force is negative for compression in the force/torque (FT) sensor's co-ordinate system and this convention was preserved when modelling.

IV. Results and Discussions

A. *Experimental Results*

Figure 3 shows the results of one of the indentation tests. It can be seen that the indentation depth alone is insufficient to accurately model the force observed. The amplitude of the noise in the FT sensor was analysed to determine a lower limit for model performance, since neural networks are often prone to overfitting noise in training data. Figure 4 shows the filtered force response from the FT sensor in a 5 minute period of no load with an approximate sample period of 4 ms.

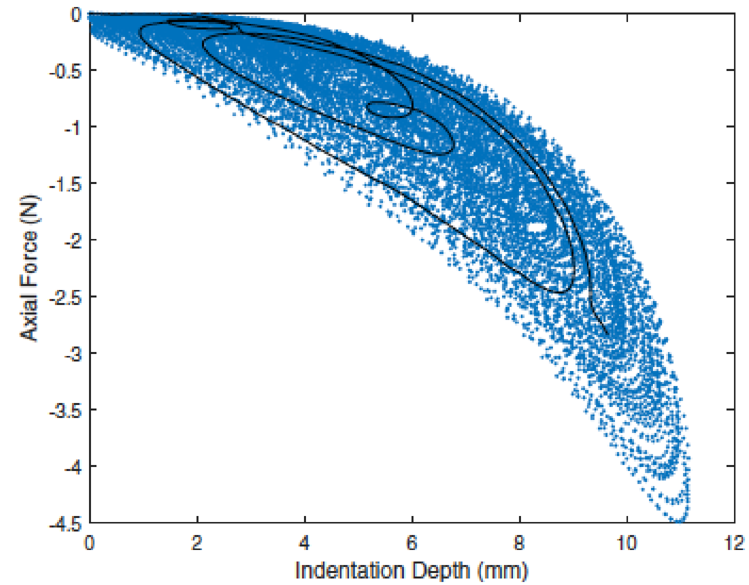

Fig. 3. Experimental force-indentation data showing the wide spread of forces at each indentation depth. The black line shows the results of the first 10 indentations.

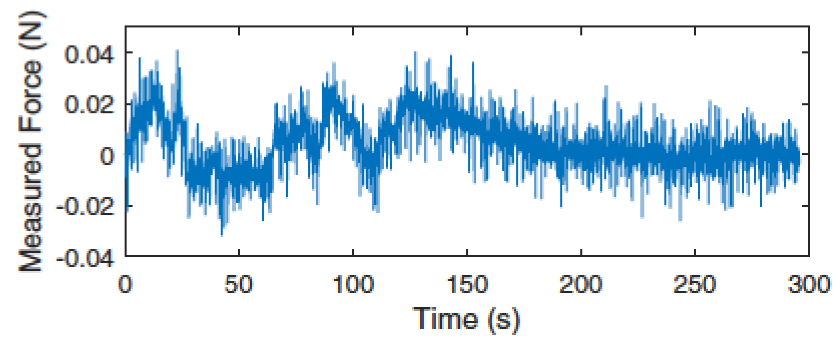

Fig. 4. Force reading from the ATI Force sensor under no external loading showing the extent of noise.

The amount of high frequency noise in the filtered measurements was calculated by taking a moving average with a 1001 sample window as a baseline and then taking the standard deviation of the difference. The standard deviation of the noise is 0.0042 N. This is important for neural network training as it sets a lower limit for acceptable error. If a neural network modelled training data with a root mean squared error below this it was considered overfitted, and training was halted. The maximum peak to peak values over this test was 0.0987 N.

Experimental results verify the non-uniformity of the tissue sample. The maximum measured axial force for 25 different locations on the sample is shown in figure 5. Because of the non linear force response of the tissue, a linear elasticity based parametrisation is not suitable. Developing a neural network model which can account for the indentation location would require the network to be trained on a case by case basis, using large sets of training data. As a compromise, a hybrid model of a neural network and the inverse strain model was developed. This model is described in section IV-C.

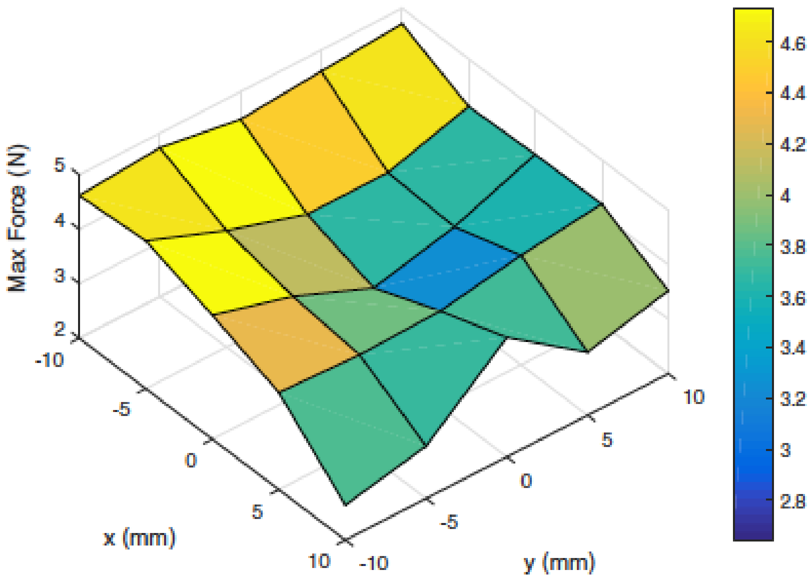

Fig. 5. Maximum force response over a 5 × 5 mm grid on the surface of the tissue analogue. The indentation test locations occur at the surface vertices.

Identify the terms: Encoder ticks

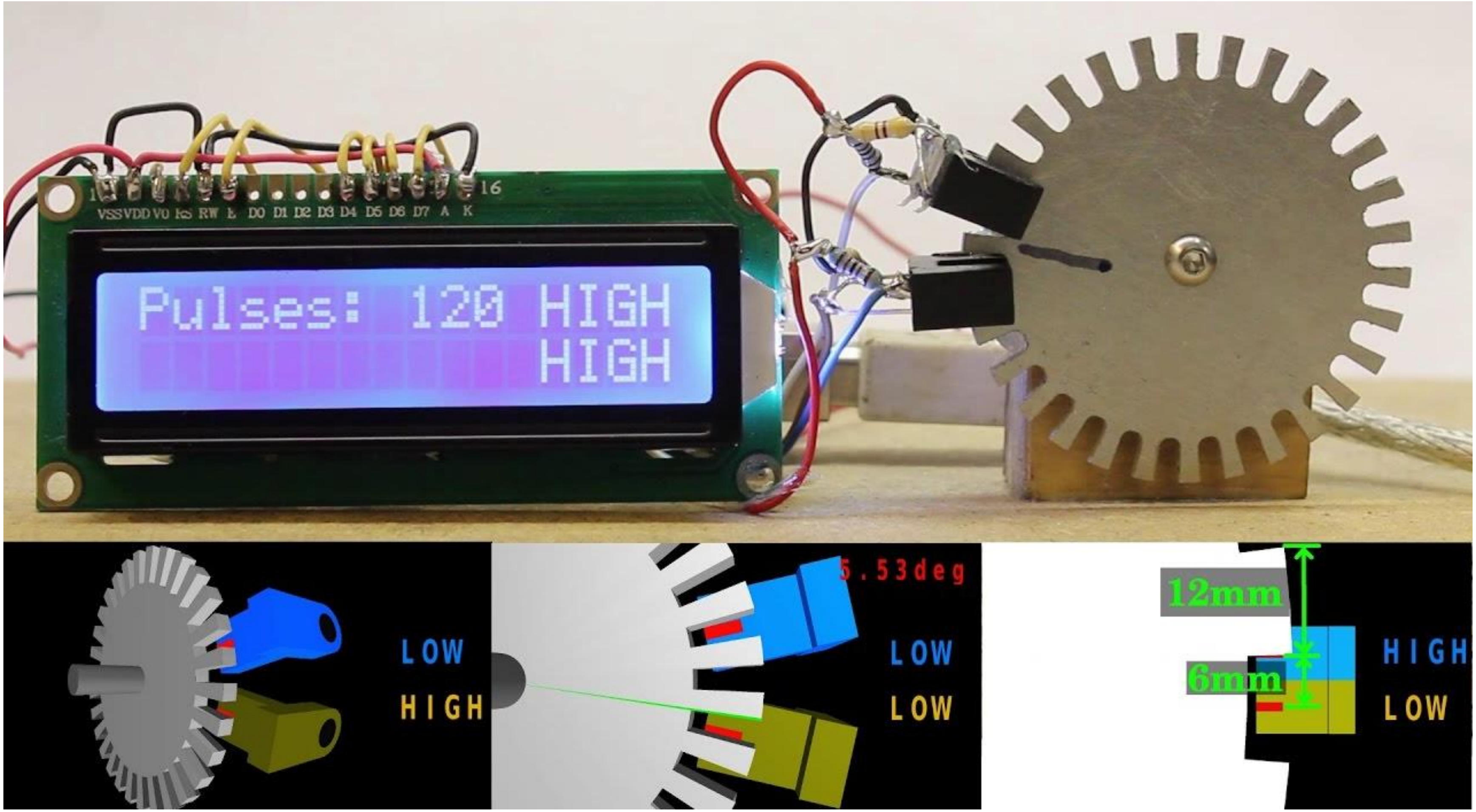

Wrist Force/Torque Sensors

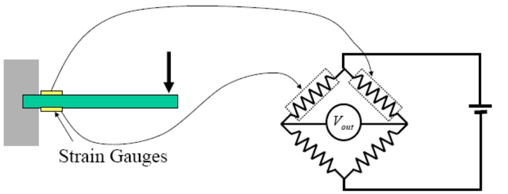

Temperature-Compensated Wheatstone Bridge

Example force / torque measurements

- 4 times 2 pairs of strain gauges
- +/- 100 N force
- +/- 10 Nm torque
- 1% precsion (from max value)
- Resolution 10^-4

6-Axis Wrist Force/Torque Se

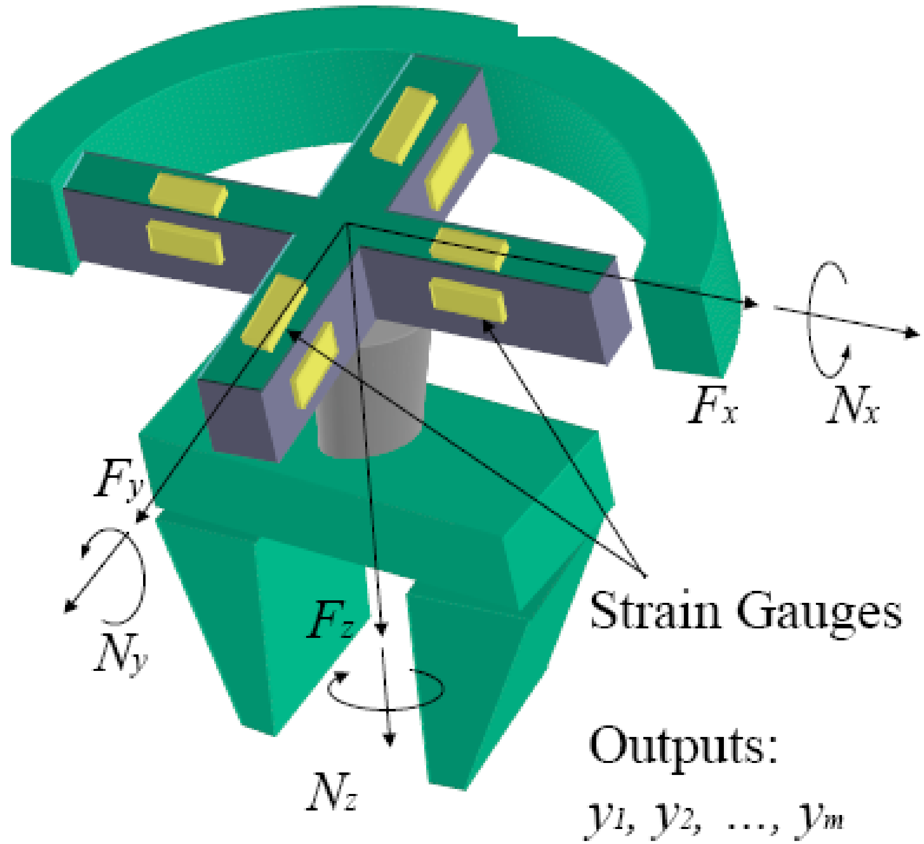

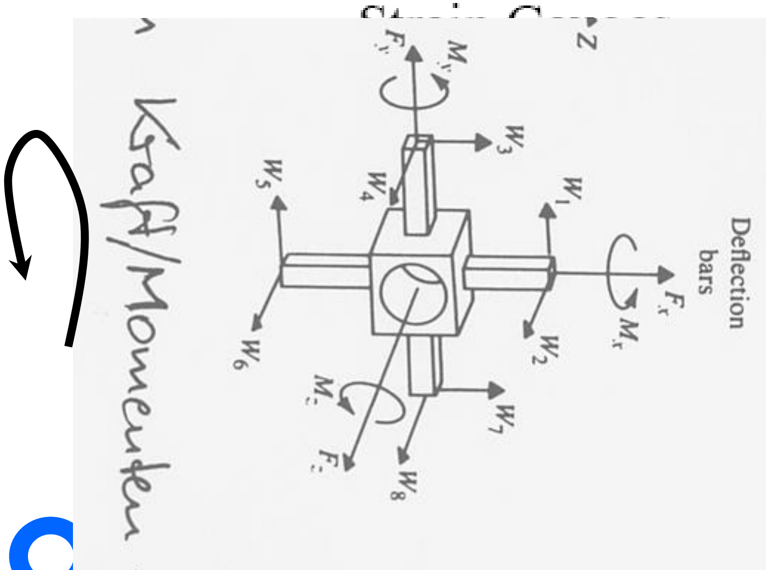

2B:Example Methods

Methods:

- deflection of armatur
- compensation

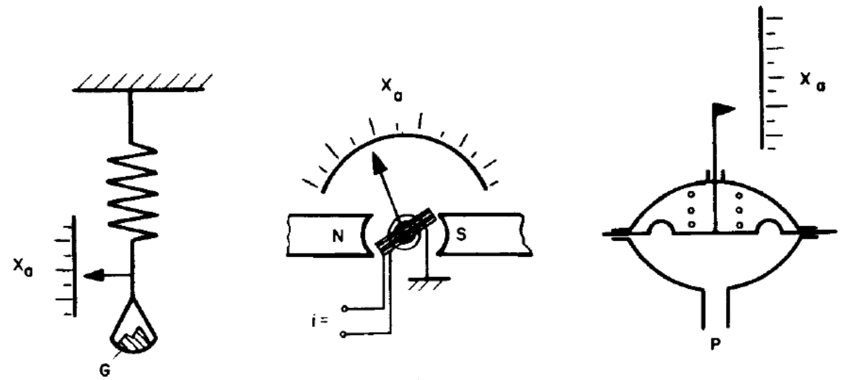

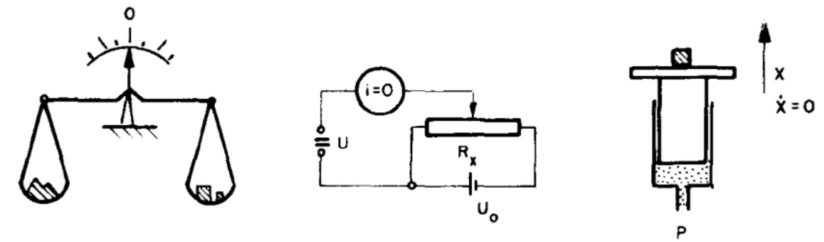

2B Quick check (10min)

Assume: it‘s a nice and very hot summer day and you like to measure the temperature of your desk at home while working.

- Apply the general formalized terms to this experiment
- What is measurand, what is DUT?
- ....

2B: Accuracy and Precision

x_t true value (reference, true grd), i.g. unknown, e.g. distance too wall

x_b “best“ value, as close as we can get (assume: error free measurement, approximated by expected value $\mu \approx \bar{x}$, „right“ value)

x_a “angezeigter“ value, as currently displayed

x_t $x_a \approx x_b$

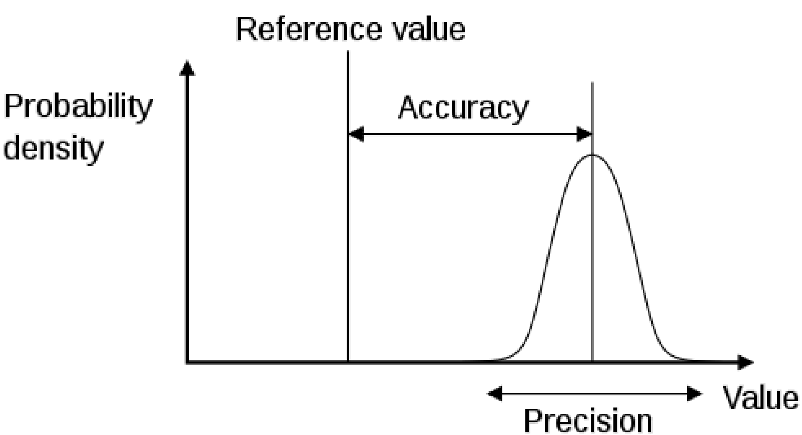

Remark: earlier we bound this distribution by the term uncertainity δ.

(Measurement) accuracy

closeness of agreement between a measured quantity value and a true quantity value of a measurand.

(Measurement) precision (distribution)

closeness of agreement between indications or measured quantity values obtained by replicate measurements on the same or similar objects under specified conditions.

Precision is used to define measurement repeatability, intermediate measurement precision, and measurement reproducibility. Sometimes “measurement precision” is erroneously used to indicate measurement accuracy.

2E: Systematic and Random Errors Absolut error and relative Error

Any repetitive measurement shows two types of errors:

E_s := **systematic error**

E_{ai} := **random error**.

$$E_s = \mu - x_t$$

$$E_{a_i} = x_{a_i} - \mu$$

absolute error: $\Delta_{ai} := |x_{ai} - x_t|$

relative error : $\rho_{ai} := \Delta_{ai} / x_t$

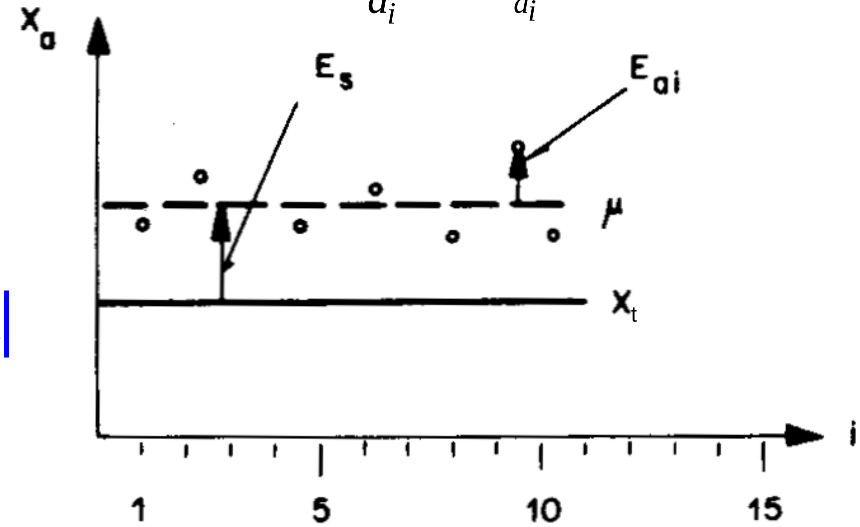

trial number (count)

2E Significant Figures notation

$c = (2.99792 \pm 0.00030) \cdot 10^8$ m/s

(extended notation)

$c = (0.299792 \pm 0.000030)$ Gm/s

(extended notation with unit prefix)

$c = 2.99792(30) \cdot 10^8$ m/s

(concise notation)

All intervals relate to the **absolute error** Δ_{ai} of the measurement

2E Quick check (10min)

Assume: it‘s a nice and very hot summer day and you happen to have a tape measure from metal. You a trying to measure the length of the classroom and the tape measure stayed on the window sill all day.

- When you now actually measure the length which kind error will you observe?
- Will it be positive or negative? Why?
- Can we cure it? How?
- What SIZES do you expect?

Example

2E: Interplay: Systematic vs. Random

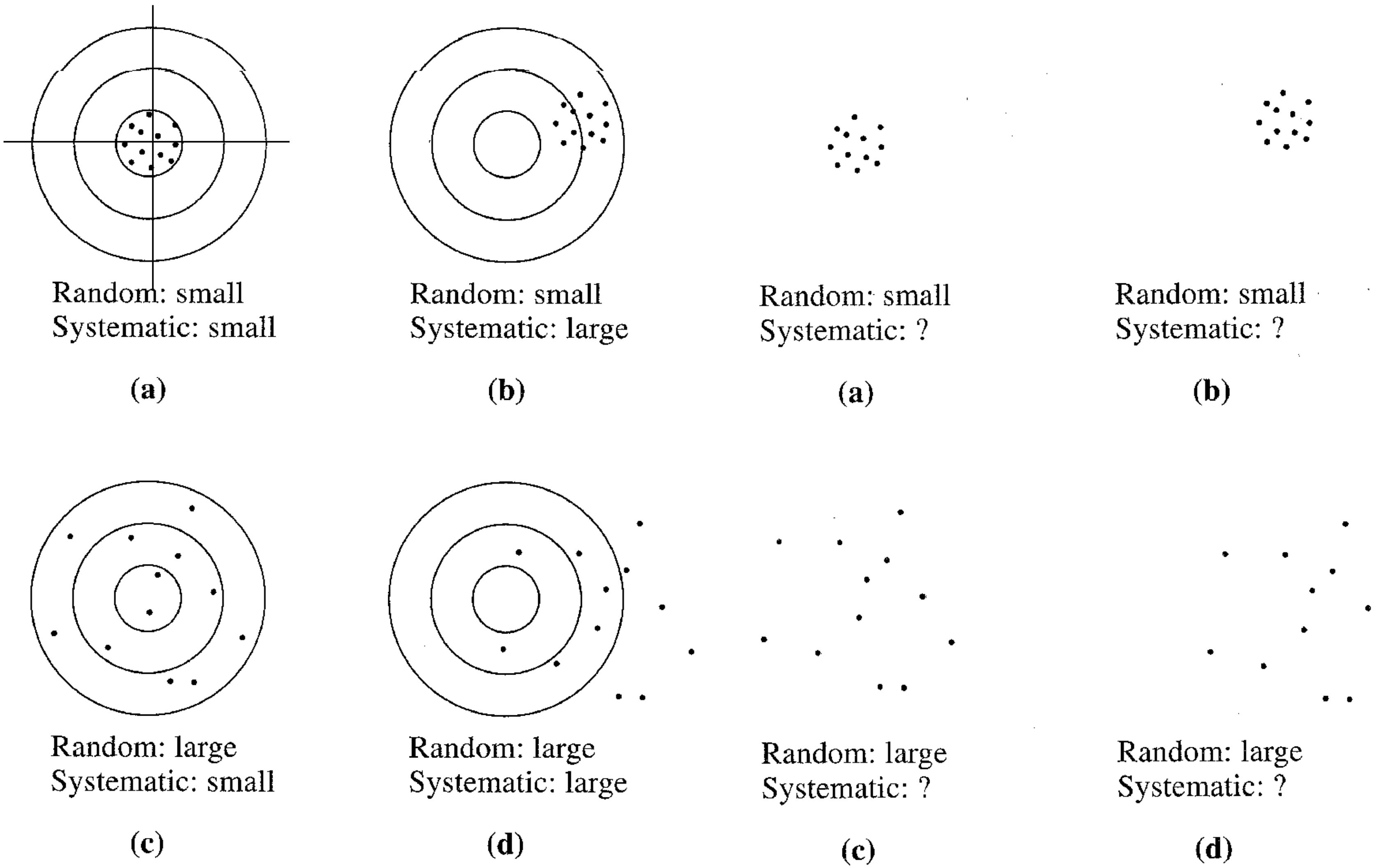

Target known => can judge systematic errors
target unknown => only random errors can be judged

shoots to a known / unknown target

2E: How to estimate x_b?

Do repeated empirical measurements => use samples

The empirical expectation is called “sample mean value”
similar: empirical variance S_x (“S”treuung or “S”catter):

$$\bar{x}_{an} = \frac{1}{n}\sum_{i=1}^{n} x_{ai}$$

$$S_{xa}^2 = \frac{1}{n-1}\sum_{i=1}^{n} (x_{ai} - \bar{x}_n)^2$$

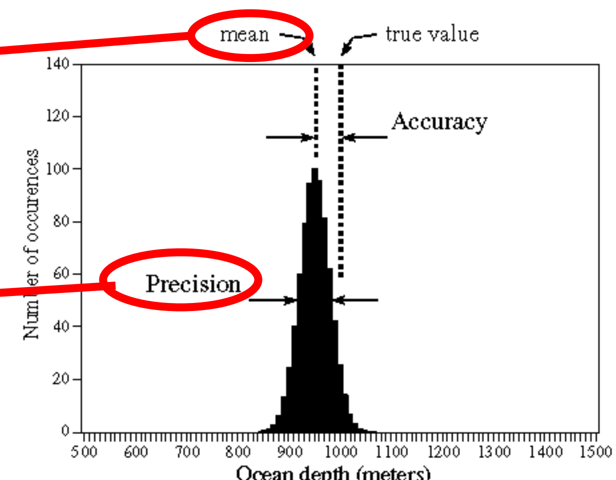

One can show: these are optimal estimators (maximum likelihood estimators)

Furthermore for the expected value μ:

$$\mu = \lim_{n\to\infty} \frac{1}{n}\sum_{i=1}^{n} x_i$$

Precision depends of the meter (repeatability).

Accuracy depends on all components of the measurement facility.

2E: we may **cure** systematic errors E_s **by calibration**

E_s can be repeated, every time it is the same thus it is a deterministic error.

- caused by factors that can (in theory) be modeled -> prediction
- e.g. **calibration** of a laser sensor
- e.g. distortion caused by the optic of a camera

E_{ai} is a random error -> non-deterministic

- no prediction possible
- however, they can be described probabilistically
- e.g. Hue, instability of camera, black level noise of camera .

Calibration:

An illustrative example is the calibration of a self-indicating weighing by putting of normalized weights. Taking into account systematic effects (previously determined by calibration measurement deviations of the weights, air pressure, temperature, buoyancy forces) and random influences the display of the scale is compared with the launched mass and then we estimate the uncertainty of this deviation.
A simple calibration result is: The weight displays at a load of 200 g, a deviation of +0.12 g, this result has an uncertainty of 0.20 g with a confidence interval of 95%.

(wikipedia on Calibration)

2E: example calibration

a

b

Fig. 7.6. **Radial distortion correction.** *(a) The original image with lines which are straight in the world, but curved in the image. Several of these lines are annotated by dashed curves. (b) The image warped to remove the radial distortion. Note that the lines in the periphery of the image are now straight, but that the boundary of the image is curved.*

Observation

A theorem at the heart of nature: A Numerical Experiment on the Central Limit Theorem

```
close all; clear;
```

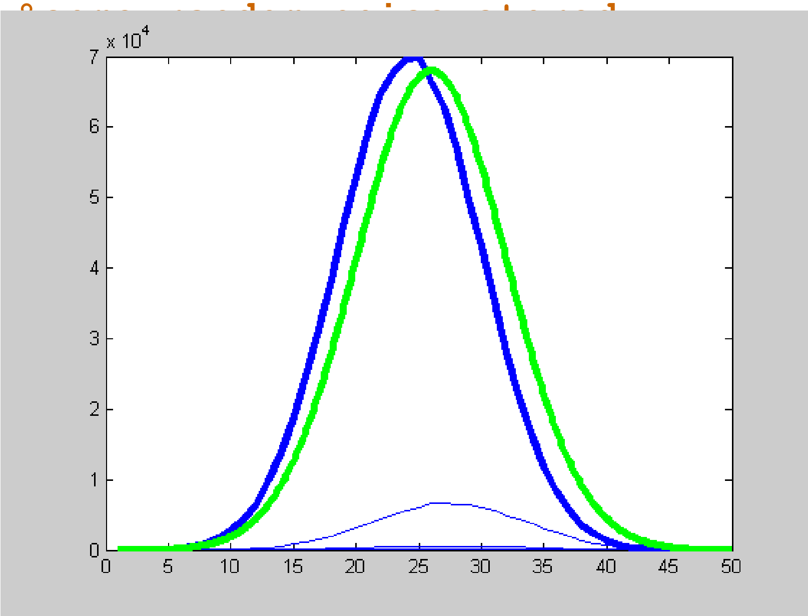


```
A(2,:))/2,'b'),plot(...
 (A(1,:)+A(2,:)+A(3,:)+A(4,:))...
/4,'g')
pause
%use build in MATLAB function
plot(mean(A))
pause
```

```
%divide range into 50 equidistant
%classes and count the members
A=rand(12,1000);
plot(hist(mean(A),50))
pause
%make more precise by higher sample count
hold on
A=rand(12,10000);...
        plot(hist(mean(A),50));pause
A=rand(12,100000);...
        plot(hist(mean(A),50));pause
A=rand(12,1000000);...
        plot(hist(mean(A),50));pause
%compare to a very special functionm
t=1:0.1:50;
plot(t,6.8e4*exp(-(t-26).*(t-
26)./(2*6*6)),'g')
```

MATLAB

1) Noise is not completely arbitrary, rather it contains some hidden regularity i.e. the Gaussian bell shaped function
2) This is the actual reason why repetitions of measurements will eventually converge to the true values!
3) The math behind it: central limit theorem

2D: $\bar{x}_{an}$ is Normally distributed

By central limit theorem:

If we repeat measurements with same instrument very often (I.I.D.) AND sum and build averages, then we are arbitrary close to a normal distribution

$$\lim_{n\to\infty} \bar{x}_{an} = \frac{X_1 + \cdots + X_n}{n} \to \frac{1}{\sigma\sqrt{2\pi}} e^{-\frac{(x-\mu)^2}{2\sigma^2}}$$

2D: Normal (Gaussian) distr.

$$f(t) = \frac{1}{\sigma\sqrt{2\pi}} e^{-\frac{1}{2}\frac{(t-\mu)^2}{\sigma^2}}$$

abbreviated to

$$x \sim N(\mu, \sigma^2)$$

$$F(x) = \int_{-\infty}^{x} f(t)\,dt$$

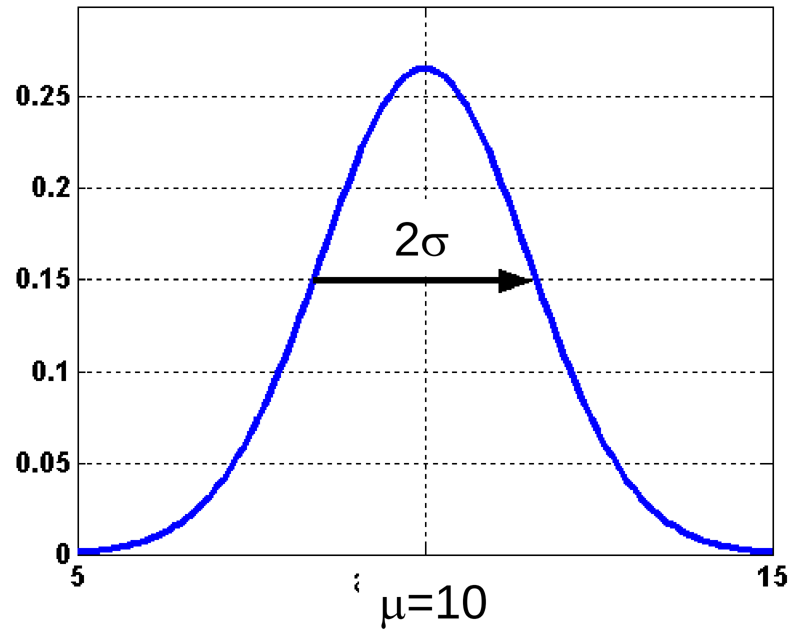

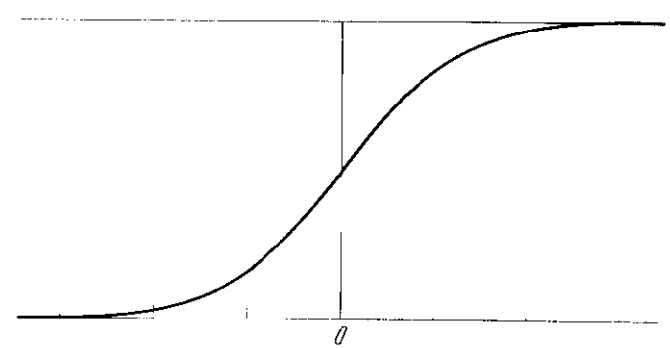

Fig. 2. Gaussian error function

2D: Examples of 2 Gaussians

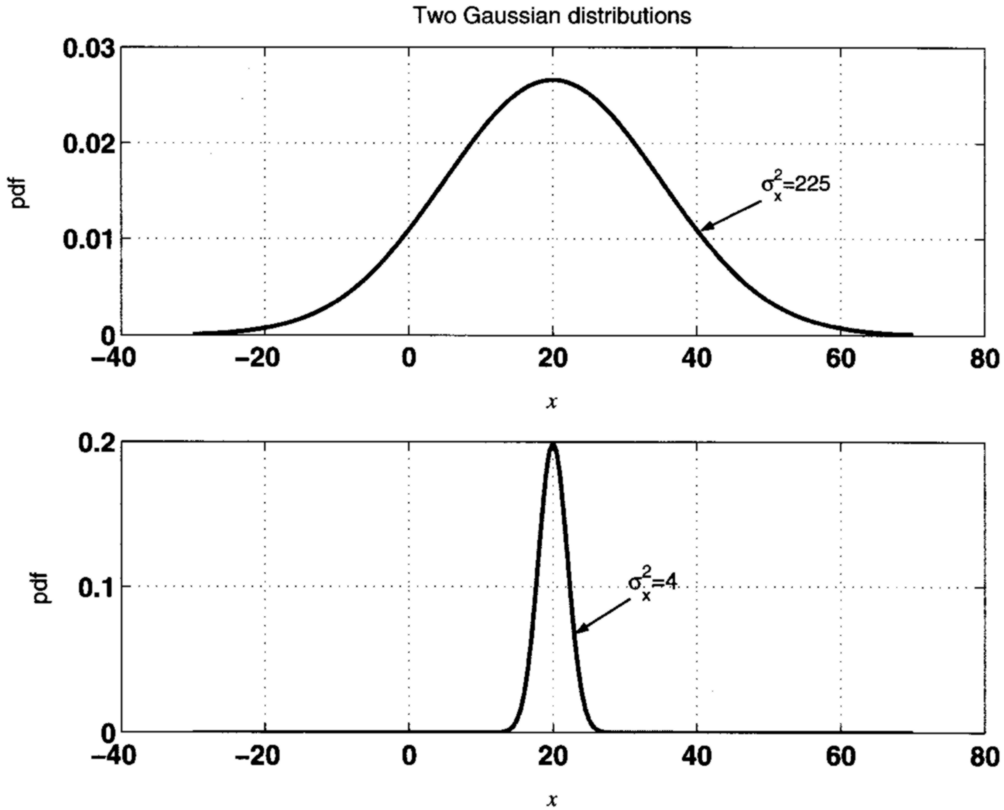

Figure 1.1. The figure shows the plots of the probability density functions of a Gaussian random variable $\boldsymbol{x}$ with mean $\bar{x} = 20$, variance $\sigma_x^2 = 225$ in the top plot, and variance $\sigma_x^2 = 4$ in the bottom plot.

2D: higher dimensional N(μ,σ)

```
mu = [0 0];
Sigma = [.25 .3; .3 1];
x1 = -3:.2:3; x2 = -3:.2:3;
[X1,X2] = meshgrid(x1,x2);
F = mvnpdf([X1(:) X2(:)],mu,Sigma);
F = reshape(F,length(x2),length(x1));
surf(x1,x2,F);
caxis([min(F(:))-.5*range(F(:)),max(F(:))]);
axis([-3 3 -3 3 0 .4])
xlabel('x1'); ylabel('x2');
zlabel('Probability Density');
```

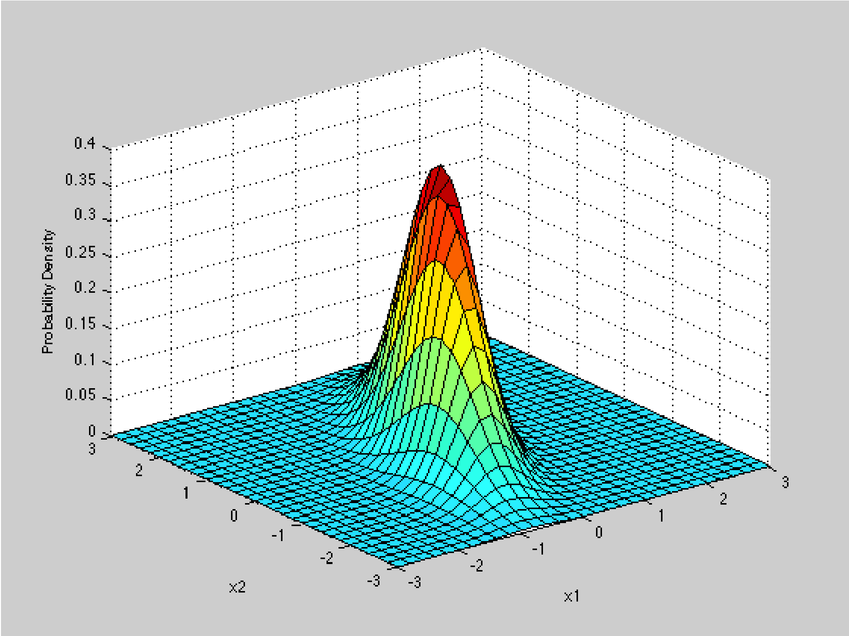

Example

2D: If N(μ,σ) is known ...

…. we then can apply a statistical test, to determine how likely a given measurement value x_i may actually be an outlier !

Since we make a statement on a random experiment a likelihood bound (p%) needs to be given.

E.g: if we want to be sure at level e.g. p = 95% that x_i is an inlier, what is the bound for x_i?

2D: If N(μ,σ) is known ...

Define the confidence level of x_i: $\mathbf{P}(|x_i - \mu| < c)$

Read this as the likelihood, that distance from x_i to μ is less then c.
=> shaded area under Gauss distribution(integral)

Method: remap the given likelihood (0.95) back to multiples of σ,
here: 0.95 <- 1.9

Thus an x_i which is farer away form μ then 1.9σ is an outlier in 95% of all cases.

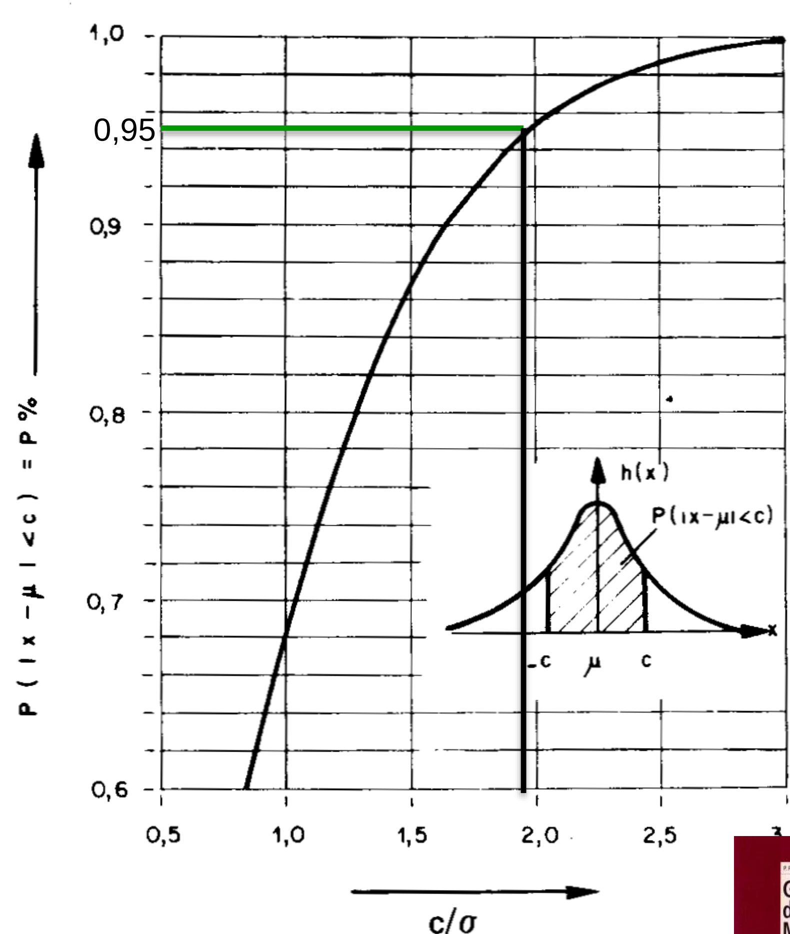

$1{,}9 = c/\sigma \Rightarrow c = 1.9\sigma$

Example

2D: testing for N(μ,σ)

Chi square test:

a) From n sample values (from an underlying totality following some hidden distribution D) build estimators $\bar{x}_n$ and S_x !

b) Subdivide all n samples into K classes ($K >= 4$) s.t. in each class there are at least 5 samples (width of class may vary if necessary).

c) Get n_{ei}, i.e. the observed number of samples per class i.

d) Build $N(\bar{x}_n,S_x)$ and P_i, i.e. the likelihood that a sample lies in class i, then build $n_{oi}=P_i*n$, i.e. the number of to-be-expected samples in class i if the totality would be distributed according to $N(\bar{x}_n,S_x)$.

e) Build χ^2 and $n_f = K-1$.

$$\bar{x}_n = \frac{1}{n}\sum_{i=1}^{n} x_i \quad S_x = \sqrt{\frac{1}{n-1}\sum_{i} (x_i - \bar{x}_n)^2} \qquad \chi^2 = \sum_{i=1}^{K} \frac{(n_{ei} - n_{oi})^2}{n_{oi}}$$

Example

2D: testing for N(μ,σ)

If point (χ^2, n_f) lies in non-hashed area, there is no indication, that D would NOT be normal (up to a confidence level of 5% below and above)

NB:

This test works for ANY distribution! E.g. uniform etc

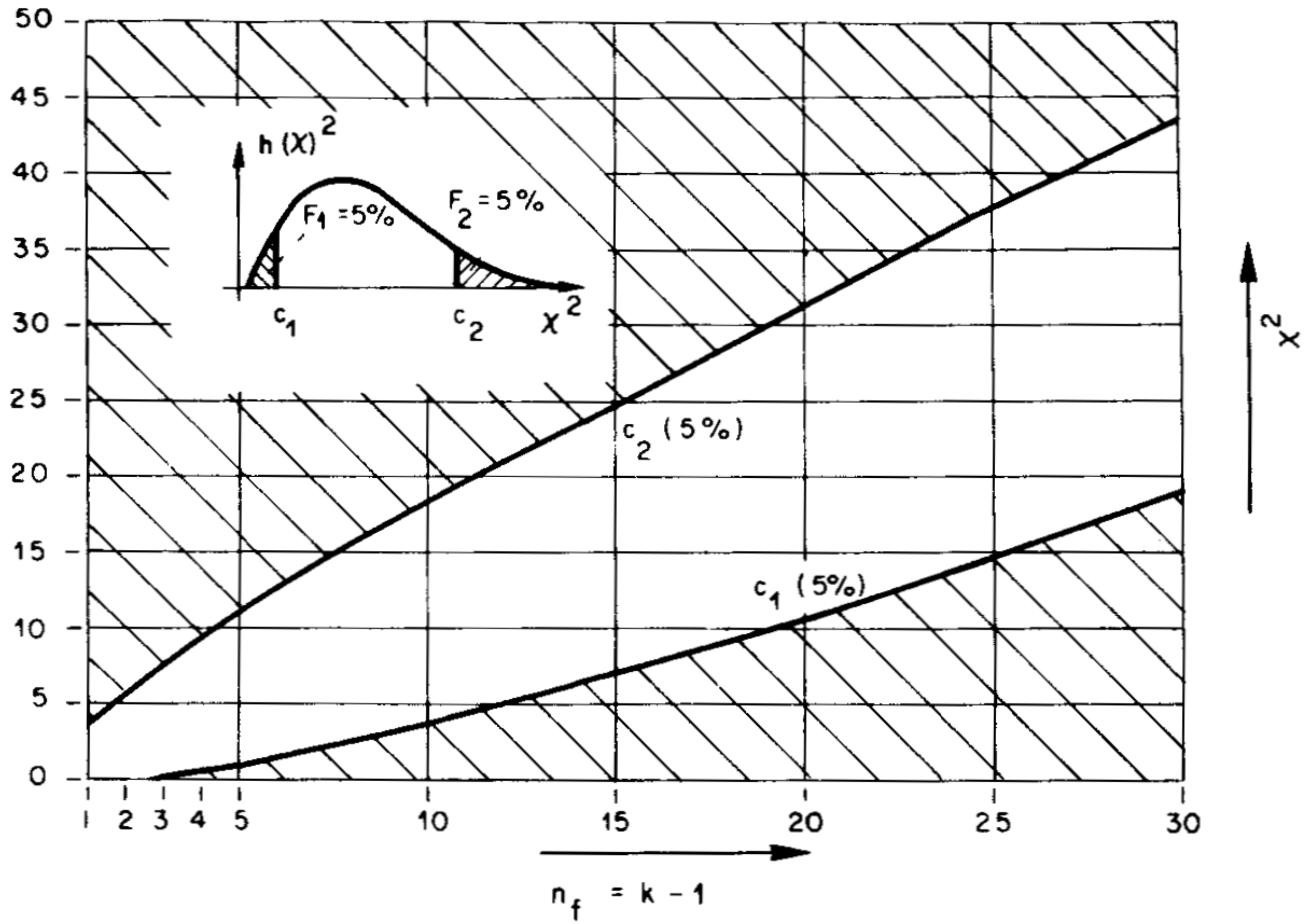

3 Summary

- Measurements suffer from many effects (**random** and/or **systematic**).
- **Systematic errors** may be cured by **calibration**.
- **Random errors** are not totally random, there is distribution underneath (**mostly: Gaussian**, also in higher dimensions)
- **Sampling and averaging** helps to read „richtige“ **values x_r** (empirical mean and spread)
- **Distributions** may be checked versus model distributions **using χ^2 test.**

Example and Homework

The following is a recent published example for the description of an experimental setup.

How detailed is the example decribed, can we rerun the experiment with equal results?

What is missing (if so...) ?

Apply the **Formalized General terms** to this setup!

3.1 Setup

digital micromirror device (DMD)

A phase-SLM is another type of spatial light modulator

Ivan Vishniakou's
Master thesis

3.1.1 Optics

Several versions of the setup have been developed for the work described in this thesis. The optics of the first setup that we used for scattering control is described in detail in [49] and shown schematically in figure 3.3 a. Briefly, a laser beam is expanded with a pair of lenses and reflected by a spatial light modulator (DMD); then the modulated beam is imaged through the scattering sample. Transmitted and reflected light is collected and recorded with CMOS cameras. The scattering sample is mounted on a x- y- z- motor-actuated translation stage, which allows displacing the sample to focus in different locations or fields-of-view (FOVs).

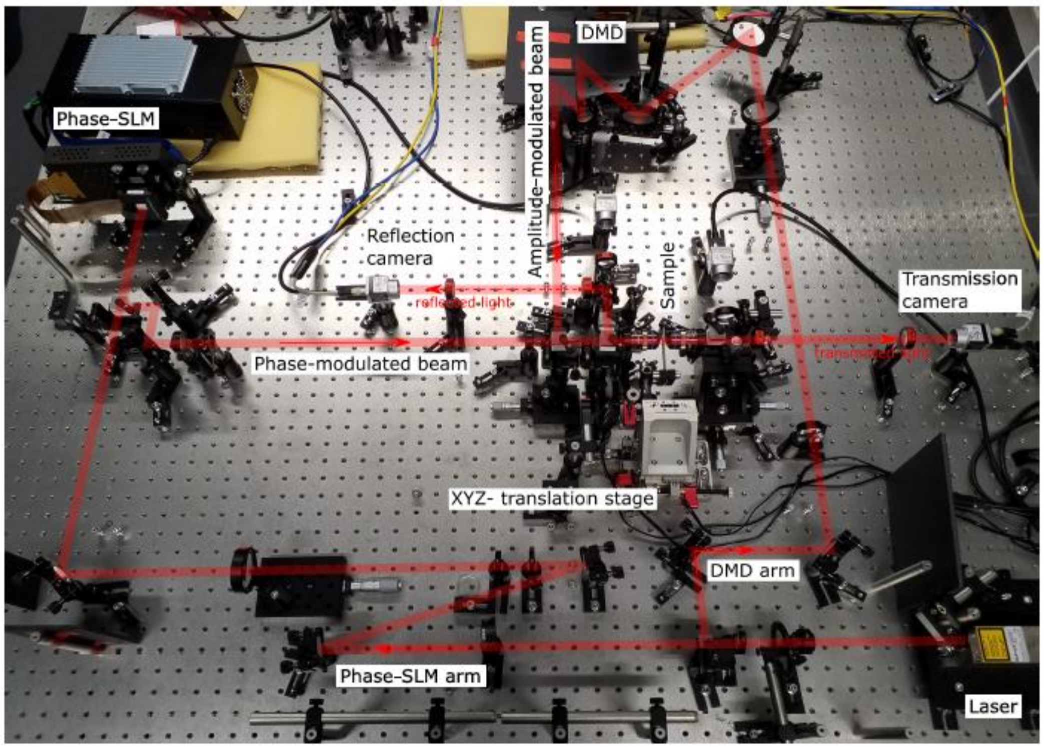

Figure 3.1: Picture of the experimental setup. Two parallel beam paths allow to use either the phase-SLM or the DMD to modulate light (see schematics in figure 3.3).

After an initial series of experiments, several changes were made in the context of the work discussed in this thesis to improve the setup's performance in terms of enhancement and stability. First, the stability was increased by mechanically isolating the DMD and the optical table with respect to to each other. Second, by inserting an optical isolator (Thorlabs, IO-3D-633-VLP) after the laser output, back-reflections into the laser could be avoided and laser stability could be improved. Third, an objective with higher magnification and the corresponding imaging optics were inserted and aligned (Olympus 40X, 0.6 NA , WD=2.7-4.0). Fourth, spherical singlet lenses were used instead of achromatic lenses (Thorlabs) in all imaging related optical paths. The DMD (positioned in the focal plane of the first lens) is demagnified onto the backfocal plane of the microscope objective using two lenses with focal lengths f= 30 cm and 15 cm, respectively. The SLM is similarly positioned in the focal plane of another lens and demagnified onto the backfocal plane of the objective using focal lengths f = 25 and 12,5 cm, respectively. The speckles are demagnified using focal lengths f = 10 cm and 8 cm onto the camera, in transmission and reflection k-space.

Altogether, these changes contributed to a better enhancement ($\eta = 81$ ($s = 18$) compared to $\eta = 32$ ($s = 5$) before) and longer persistence time for a given correction (see chapter 5).

Additionally, a second excitation path with a phase modulating SLM was incorporated into the setup and included in the software control framework for transmission matrix measurements. The two beam path shown separately in figure 3.3 a and b were combined with a beam splitter that allows easily switching between phase and intensity modulation, as can be seen on the photo of the setup in figure 3.1.

3.1.2 Hardware

A lab workstation running on Windows was used for automated experiment control and data acquisition, with an Intel Xeon CPU E5-1660 v4@3.20 GHz, 32Gb of DDR5 RAM memory. A separate Linux-Ubuntu machine with identical specs but additionally equipped with Nvidia Titan XP GPU providing 3840 CUDA cores running at 1.60 GHz and 12GB of GDDR5X was used for machine learning methods and simulations.

3.1.3 Instrument control and interfacing

The experimental setup includes diverse hardware components that need to run in synchrony, namely image acquisition with multiple cameras and image display on either the DMD or phase-SLM. For this purpose, custom software was developed with Python using the appropriate device APIs. The implemented scripts allow the following control loops:

- Closed loop: A pattern is displayed on the SLM - the resulting speckle patterns are imaged - the result is evaluated and the SLM pattern is accordingly updated. This control loop was used for the iterative wavefront optimization methods tested. Additionally, multiple exposure times of the camera were added to increase the dynamic range of the measurements.
- Open loop: display a series of predefined SLM patterns one-by-one with set exposure settings and simultaneously record the respective speckle images.

One of the objectives in the control of the experiments was to achieve the lowest possible closed loop time and highest possible pattern throughput in open loop. This is advantageous for running wavefront optimizations within the persistence times of the correction. The factors mostly contributing to control loop iteration time are display latency of the modulation device and the camera exposure time needed to image the speckles.

The camera exposure was selected to be the shortest possible (to increase frame rate) while being sufficient to record speckles with intensity values in the range of the 8 bpp images. The camera gain was set to it's lowest value to avoid introducing additional measurement noise. The minimal exposure time satisfying these constraints with a laser power of 100 mW was found to be 5 ms.

Pattern display latency is unavoidable in closed-loop control, however, in open-loop mode, the Vialux DMD allows to run a preloaded sequence of binary patterns at rates of up to 22kHz, which is by far exceeding the imaging frame rate. Preloading of the image sequence was therefore used with TTL-pulse-synchronized free-running camera imaging, allowing for 180 frames per second (fps) pattern display and acquisition with 5 ms exposure time.

In closed-loop mode with triple exposure of 1, 2 and 5 ms for extended dynamic range an imaging rate of around 50 fps was achieved. The overall latency results from the time needed to transfer images to the DMD, to update the camera control and to adjust its exposure, as well as for the calculations of the next SLM pattern.

The Meadowlark phase-SLM does not allow for an equally fast open loop performance with preloaded patterns as the DMD, however, its interfacing through the x8 PCI Express makes this a negligible factor; the phase-SLM is intrinsically limited in frame rate by the liquid crystal latency. The resulting rate of the control loop with the phase-SLM was 7.7 Hz for interferometric measurement, which uses 4 exposures (see below).

Interferometric measurement with the SLM

Using the phase-SLM allows implementing interferometric measurements of the speckles for inferring the complex amplitude of the output light field. This is achieved in the following way: the SLM is subdivided into two parts of equal area: a reference part which displays a single phase value, and a modulation part which provides spatial modulation of the beam with different patterns. After propagating through the sample, the light from both parts is scrambled and the reference- and modulation-speckles overlap in the imaged field of view. By switching the reference part through four reference phases of (0, $\pi/2$, π and $3\pi/2$) and imaging the corresponding speckle intensities, it is possible to infer the complex amplitude induced by the modulation pattern as described in section 1.5.4.

SLM calibration

The Meadowlark phase-SLM requires calibration of the phase change at a given applied voltage for a given wavelength. It accepts 8bpp images, where each pixel value in the range from 0 to 255 corresponds to a phase delay in the range of about 0 to 2π (depending on the wavelength). The phase of each pixel is set by mapping 8-bit input values to a 16-bit voltage value applied to the corresponding LCD segment using a non-linear calibration curve via a look-up table (LUT). The device is supplied with such a calibration curve reflecting the LCD nonlinearity, however, because the phase delay induced by the LCD depends on the wavelength, calibration is needed to limit the operating range of that curve to the 0 to 2π range.

The calibration was performed using a common-path interferometer that was set up for this purpose [40, 41]. The SLM was initialized with the provided LUT and half of the SLM was displaying constant phase, while the other half displayed the modulations ranging from 0 to 255. The imaged speckles were analyzed and the intensity variation was linked to the phase offset between SLM parts via the interference equation 1.11. It turned out that the default LUT provides phase delay of more than 2π for our 640 nm laser, and therefore a calibrated LUT was created by linear interpolation of the default one to map the 0 to 255 input range to a segment of the LUT providing phase modulation between 0 and 2π (see Figure 3.2).

3.1.4 Simulation

Most experimental approaches were first tested in simulations. These simulation were performed using a published transmission matrix [36] and modulating patterns and speckle distributions were related using the mathematical model described in 3.1.4 implemented in Python with Numpy (appendix A.1).

3.2 Experimental design

The approach for all experiments described in this thesis relies on displaying a pattern on the SLM, projecting this pattern optically to the sample and monitoring the resulting scattered light distribution with one or two cameras, depending on whether only transmission or both, transmission and reflection are monitored at the same time [49].

For those methods that control the entire field of view (transmission matrix or neural network approach) a sequence of patterns (typically at least a few thousands) are displayed and the corresponding camera images are recorded typically at a few hundred Hertz, close to the maximum frame rate of the camera. The resolution of spatial light modulation patterns used in this thesis is 64×64 segments, determined by the memory requirements for processing the data sets. Since both the phase-SLM and the DMD have a much higher number of pixels, the modulation pattern is scaled to use the maximal possible area of the light modulator. The entire display and

Paul G. Plöger

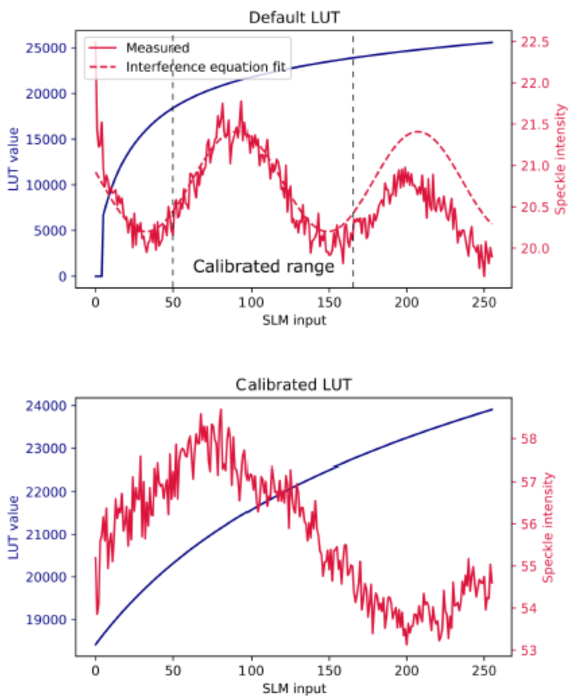

Figure 3.2: Results of SLM calibration. Using default LUT, speckle intensities were measured at different phase offsets in a common-path interferometer. The phase modulation range exceeds 2π over the 0...255 input range of the SLM (top). Calibrated LUT maps SLM input range to 2π phase modulation range, as confirmed in the measurement (bottom).

recording process was automated and could be repeated across multiple fields of view.

The sequence of displayed modulation patterns and recorded speckle patterns are then processed offline for extracting a transmission matrix or for training neural network models. Both, the transmission matrices and the neural networks offer an inverse relationship between the resulting light distributions and the displayed patterns. Feeding a desired focusing pattern into these models then results in an appropriate modulation pattern that needs to be displayed on the SLM. Due to the

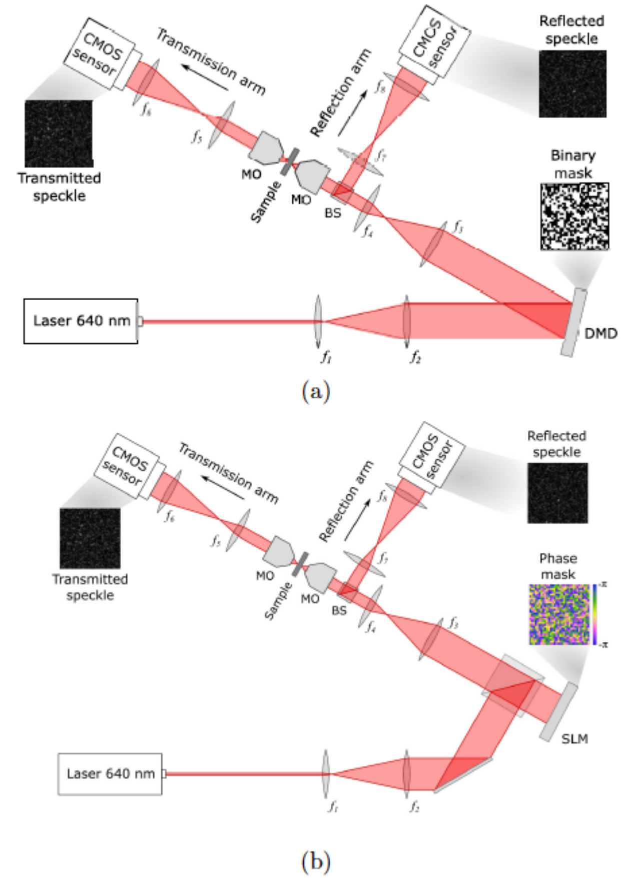

Figure 3.3: A laser beam ($\lambda = 640\,\mathrm{nm}$, with an intensity of up to $P = 100\,\mathrm{mW}$, iBeamSmart, Toptica) is expanded with a telescope ($f_1 = 15\,\mathrm{mm}$, $f_2 = 150\,\mathrm{mm}$) and sent to the DMD (a) or Phase-SLM (b). Two additional lenses ($f_3 = 200\,\mathrm{mm}$, $f_4 = 50\,\mathrm{mm}$) are used after the SLM to demagnify the beam and image it onto the back aperture of the microscope objective (MO) (10X, 0.25 NA, or 40X, 0.6 NA). The microscope objective focuses the light beam through the scattering sample, and a second identical microscope objective is used to collect the scattered light. Finally, a pair of lenses ($f_5 = 100\,\mathrm{mm}$, $f_6 = 75\,\mathrm{mm}$) images the back aperture of the second microscope objective onto the CMOS camera (acA640-750um, Basler). For experiments with reflected light, a non-polarizing beam splitter (BS) redirects the backscattered speckles towards a pair of lenses ($f_7 = 50\,\mathrm{mm}$, $f_8 = 25\,\mathrm{mm}$) that image the back aperture of the first microscope objective onto a second identical CMOS camera, synchronized with the one used to capture the transmitted speckles (reflection arm).